Observation and modeling of the time-dependent descreening of internal electric field in a wurtzite $GaN/Al_{0.15}Ga_{0.85}N$ quantum well after high photoexcitation

P. Lefebvre, S. Kalliakos, T. Bretagnon, P. Valvin, T. Taliercio, and B. Gil
Groupe d'Etude des Semiconducteurs, CNRS, Université Montpellier II, Case Courrier 074, 34095 Montpellier Cedex 5, France

N. Grandjean and J. Massies
Centre de Recherche sur l'Hétéro-Epitaxie et ses Applications, CNRS, Rue Bernard Grégory, 06560 Valbonne, France
(Received 23 July 2003; published 12 January 2004)

We use the intense, 5-ns-long, excitation pulses provided by the fourth harmonic of a neodymium-doped yttrium aluminum garnet (Nd:YAG) laser to induce a strong high-energy shift of the photoluminescence of a 7.8-nm-wide $GaN/Al_{0.15}Ga_{0.85}N$ single quantum well. We follow the complex relaxation dynamics of the energy and of the intensity of this emission, by using a time-resolved photoluminescence setup. We obtain excellent agreement between our experimental results and those of our finite-element modeling of the time-dependent energy and oscillator strength. The model, based on a self-consistent solution of the Schrödinger and Poisson equations, accounts for the three important sources of energy shifts: (1) the screening of the electric field present along the growth axis of the well, by accumulation of electron-hole dipoles, (2) the band-gap renormalization induced by many-body interactions, and (3) the filling of the conduction and valence bands.

DOI: 10.1103/PhysRevB.69.035307 PACS number(s): 78.47.+p, 78.67.De, 78.55.Cr, 73.21.Fg

I. INTRODUCTION

Quantum wells (QWs) and quantum dots (QDs) based on hexagonal (wurtzite) group-III nitride semiconductors exhibit an original property: the existence of huge internal electric fields along the (0001) growth axis.[1–11] Such fields are induced by the difference in spontaneous and piezoelectric polarization between the well and barrier materials.[3,4] The reported values of electric fields in GaN/(Al,Ga)N,[5,6] (Ga,In)N/GaN,[7–10] or GaN/AlN (Ref. 11) nanostructures are larger by one order of magnitude than those obtained earlier for QWs made of zinc blende crystals, grown along the (111) direction, like (Ga,In)As/GaAs (Refs. 12–14) or CdTe/(Cd,Zn)Te QWs.[15] As for linear optical properties of nitride QWs and QDs, the electric field is so strong that it cannot be considered as a small perturbation of the quantum confinement, slightly redshifting the ground-state optical transition and reducing its oscillator strength (the ''quantum-confined Stark effect''). Instead, we may rather state that the confinement induced by the presence of potential barriers comes as a perturbation of a giant electric field effect, a situation that some authors[16] proposed to call the ''quantum-confined Franz-Keldysh effect.'' As a matter of fact, the field is often so strong that the energy of the fundamental excitonic transition falls below the excitonic gap of the well material, for QW widths larger than 10–12 atomic monolayers (MLs), typically[17] (1 ML = 0.259 nm, for unstrained GaN).

Another important consequence of electric fields in QWs, regardless of whether these fields are internal or externally applied, is the possibility to induce a specific, often nonlinear, optical response, by using high-intensity laser excitation. Such effects have been predicted to result from the creation of a dense population of real[18–20] or even virtual[21–24] electron-hole (*e-h*) pairs. The case of high densities of real *e-h* pairs, created by absorption of photons above the band gap of the system, has been investigated in detail by continuous-wave (cw) optical experiments on (111)-grown (Ga,In)As/GaAs QWs,[14,25] and, more recently, by cw and time-resolved spectroscopy on wurtzite nitride QWs.[26–35] In practice, intricate physical mechanisms contribute to the observed changes in emission spectra.

First, for exciton densities larger than the Mott density, the *e-h* Coulomb attraction is screened, yielding a blueshift of the photoluminescence (PL) line equivalent to the binding energy of the confined exciton.[36,37] This blueshift is thus limited to the range of 15–25 meV for (Ga,In)As/GaAs QWs. For group-III nitrides, variational calculations reveal that the binding energy may reach 45–50 meV, for very narrow QWs (below ~2 nm),[36,37] but that the electric fields usually reduce this energy well below 35 meV, for QW widths larger than 10 ML, typically.

Second, the filling of conduction and valence subbands, by electrons and holes, shifts the PL line toward higher energies. For comparable densities of *e-h* pairs, this blueshift is larger for materials with small effective masses, since the two-dimensional densities of states are proportional to these masses.[38] For group-III nitride QWs, the densities of states are thus larger by a factor of 3–4 than those of (Ga,In)As/GaAs QWs. Consequently, the band-filling contribution is smaller by the same factor.

Third, it has been realized in previous work that high *e-h* pair densities necessarily induce complex many-body interactions, which result in the so-called ''band-gap renormalization'' (BGR) process, i.e., essentially a lowering of the overall band gap of the system. The modeling of these effects is complicated, but some theoretical attempts exist that provide quantitative estimations of this redshift, for nitride QWs.[39,40]

Fourth, and most important, the electric field separates the electron and hole wave functions toward either side of the QW. In the case of high densities of *e-h* pairs, this separation leads to an accumulation of dipoles that counteract the internal electric field: this is the so-called screening of the electric field. This effect has been investigated both theoretically and experimentally on a variety of systems, including group-III

nitrides.[27,32–35,41–43] The resulting blueshift of the emission line has already been observed in GaN/AlGaN,[26,28,29,31,33,35] and (Ga,In)N- (Refs. 27,32,34) or (Al,Ga,In)N-based QWs. The screening of the electric field also decreases the *e-h* spatial separation along the well axis, which enhances the *e-h* overlap integral, thus decreasing the radiative lifetime. This effect has already been predicted by theoretical models[41–43] and experimentally observed.[26,27,34,35]

However, what is still lacking today is a detailed experimental and theoretical study of the dynamical properties of a nitride-based QW where the electric field screening is clearly unraveled from other effects, i.e., where the time decay of blueshifts larger than a few tens of meV is observed and modeled. Up to now, such large blueshifts have been measured only by continuous-wave experiments.[28–33] Only a few papers have reported time-resolved studies, limited to rather small blueshifts.[26,27,34,35] Detailed theoretical studies of the overall dynamics (neglecting the BGR) were proposed in such cases,[35] but the amplitude of the fitted time-dependent energy shift (7 meV) was much too small to be solely assigned to the electric field screening.

In this paper, we present time-resolved photoluminescence studies of high photo-excitation effects on a purposely designed $GaN/Al_{0.15}Ga_{0.85}N$ QW. We observe a time-decaying blueshift starting from 0.2 eV. We obtain excellent agreement between the measured time-dependent emission energy and intensity with the results of our envelope function calculations.

II. EXPERIMENTAL DETAILS

The main features of our $GaN/Al_{0.15}Ga_{0.85}N$ QW are similar to those described in previous studies:[5,6] the sample was grown by molecular beam epitaxy on a sapphire substrate, followed by a $\sim$2-μm-thick GaN buffer layer. Then the quantum structure itself was deposited, consisting of a 30-nm-thick $Al_{0.15}Ga_{0.85}N$ barrier, a 30-ML-wide ($\sim$8 nm) QW, and a 30-nm-thick $Al_{0.15}Ga_{0.85}N$ cap layer. Compared to samples studied in previous papers, this QW should be regarded as very wide, i.e., we should expect the recombination energy to be much lower than the band gap of GaN. Moreover, the PL decay time should be much larger than the 5 ns obtained for a 16-ML-wide $GaN/Al_{0.17}Ga_{0.83}N$ QW, nearly isolated by 50-nm-wide barriers (this decay time was proved to be very close to the radiative lifetime of excitons, in this case, due to the minimization of the nonradiative escape of excitons out of the QW). In fact, scaling the latter radiative decay time by the calculated ratio of electron-hole envelope function overlap integrals in these two cases (the 16 ML QW of Ref. 44 and our 30 ML QW), we end up with an estimated radiative lifetime, in our sample, of $\sim$1.64 μs. This slow recombination time was one of the reasons for our choice of a wide QW, since it allows us to accumulate large densities of *e-h* pairs using reasonably small laser intensities. Also, the quantum confined Stark effect is more important in wide quantum wells and its cancellation will provoke a higher blueshift of the transition energies.

As a matter of fact, for a really comprehensive study of electric field screening effects, we need to produce energy shifts that are larger than all other possible sources of blueshift. In practice, the shifts that we observe and comment on below are larger by one order of magnitude than the exciton binding energy of 13 meV that we estimate by using a variational calculation.[45] This small value is another consequence of the strong electric field and of the large well width. Previous work[46–48] also teaches us that strong exciton localization occurs in regions where the well is wider by 1 or 2 ML than its average width. The average PL maximum is situated between the two localized-exciton energies, at a position that depends strongly on small variations of the temperature and of the overall transfer dynamics between the different zones of localization. In our case, we should expect a localization-induced Stokes shift (redshift) of the average PL maximum comprised between 21 and 42 meV.[46,47] Again, our interest is in producing screening effects that will be convincingly larger than these energies.

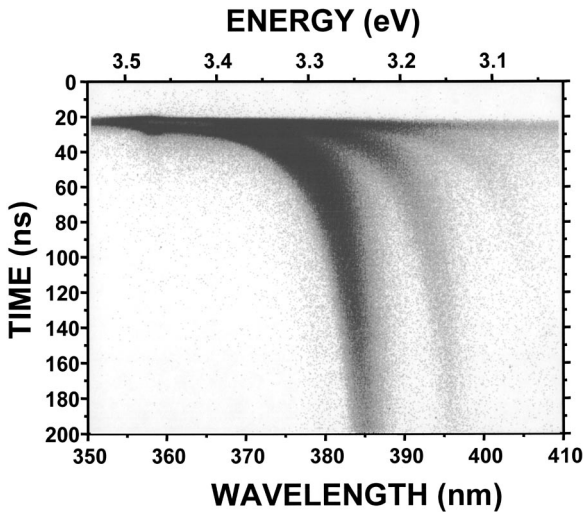

FIG. 1. Time evolution of the PL spectrum from our 30-ML-wide $GaN/Al_{0.15}Ga_{0.85}N$ quantum well, taken at $T=8$ K. Levels of gray indicate the PL intensity for a given wavelength (horizontal scale) and a given time (vertical scale). The maximum of laser excitation corresponds to time $\sim$23 ns in this picture.

For this purpose, we used the fourth harmonic ($\lambda = 260$ nm) of a pulsed neodymium-doped yttrium aluminum garnet (Nd:YAG) laser. The pulse duration was of 5 ns, with a repetition rate of 10 Hz. In practice, we produce typical average optical power densities of 2×10^{-4} W/cm^2 in the sample, i.e., a typical density of incident photons of 2.7×10^{13} cm^{-2} per pulse. The sample was placed in a closed-cycle helium refrigerator yielding a minimum temperature of 8 K. The emitted PL light was then dispersed through a monochromator and detected by a streak camera synchronized with the 10 Hz pulse train.

III. EXPERIMENTAL RESULTS

In Fig. 1 we present the streak-camera image for the time-dependent PL spectrum of our sample (N310), taken at $T = 8$ K. The excitation power density was 2×10^{-4} W/cm^2. The horizontal axis is the wavelength axis (or energy, see the top axis). The *y* axis represents the time, with the full scale

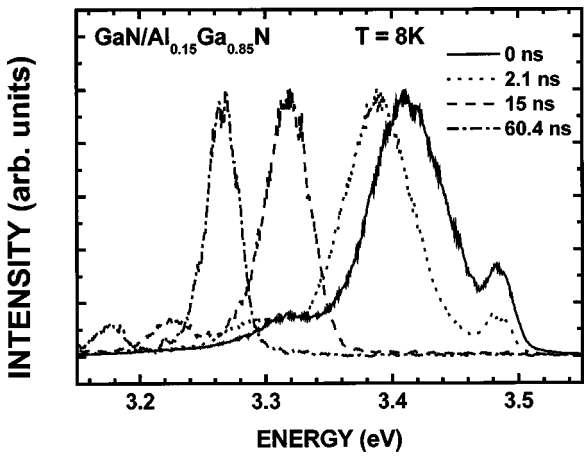

FIG. 2. Time-dependent normalized spectra of the 30 ML QW. The luminescence from the GaN buffer layer is seen only for very short delays, when we must consider that the excitation is still present, due to the relatively large duration of the laser pulse (5 ns).

corresponding to 200 ns. The ''comma shape'' of this PL signal is a clearcut image of the large blueshift of the PL, when the sample receives an intense laser excitation, followed by a time-dependent redshift, once the excitation is suppressed. This redshift and the intensity decay are both fast, just after the excitation, and they become slower and slower as time passes. This is obviously due to the increased recombination probability, at short delays, induced by the enhanced overlap integral of electron and hole envelope functions. The decrease of carrier population, because of either radiative or nonradiative recombination (mostly radiative, as well will see later), progressively restores the internal electric field and, as a consequence, the overlap integral is strongly decreased, which renders the overall dynamics of the system much slower. In addition, the first two phonon replicas can be clearly observed (the two secondary lines, separated from the main line by ~91 and ~182 meV, respectively) and we see that they follow the evolution of the main PL peak. Possible changes, with time delay, of the phonon energy and of the relative intensities of the replica are rather difficult to follow with accuracy. These points will not be discussed in this paper.

In Fig. 2 we present some intensity-normalized PL spectra extracted from the data of Fig. 1 at different time delays. For their selection, at a certain delay, we used a rectangular box that covers the whole wavelength range (x axis) with a small temporal width (y axis). The latter had to be kept small to avoid any artificial broadening and hence any distortion of the spectrum. This is specially critical at small delays, where the ''sliding'' of the overall spectrum is quite fast, because the recombination rate is much higher at smaller delays. The first two spectra in Fig. 2 were taken in conditions where the excitation pulse is still present. In these spectra, we observe, at 3.47 eV, the very short-lived PL from band-edge excitons in the GaN buffer layer.

We have fitted the time-dependent PL spectra recorded over small ''slices'' of time by using Gaussian functions that were then exploited to produce the results gathered in Fig. 3. The time-dependent redshift of the peak energy, in Fig. 3(a)

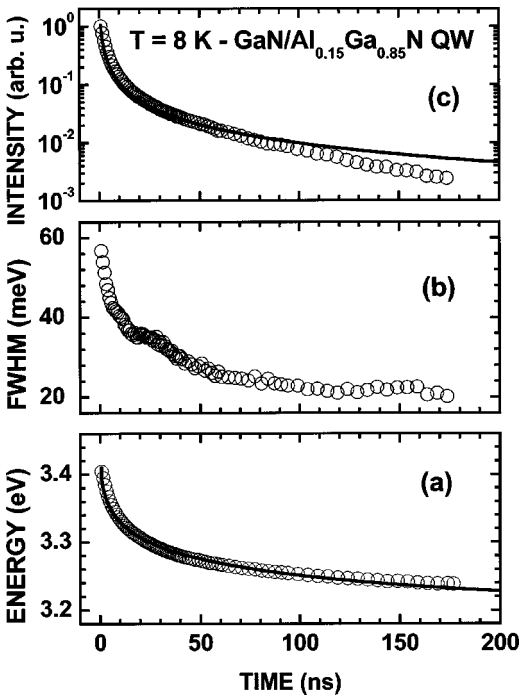

FIG. 3. Open circles show the experimental time dependence of the PL energy (a), linewidth (b), and intensity (c), extracted from spectra such as those in Fig. 2, by a fit using Gaussian functions. Solid curves show the result of our calculation.

gives an image of the time-dependent e-h pair density, since there is a one-to-one correspondence between the two quantities, as we discuss and model below. The total amplitude of this shift is ~0.2 eV, whereas the asymptotic PL energy, at large delays is ~3.23 eV. The various contributions to the PL energy shift are listed above, in the Introduction. As the spectra shift to higher energies, i.e., as we move to smaller delays, the spectrum roughly keeps the same shape, but the spectral width increases due to the band filling [Fig. 3(b)], which adds some effective contribution to the overall blueshift. Again, the linewidth decreases from ~80 to ~20 meV and this decrease is slower and slower as time passes. We calculate that the additional blueshift induced by band-filling effects becomes larger than a few meV for e-h pair densities larger than $\sim 10^{11}$ cm^{-2}. Nevertheless, the low-energy side of the spectra shown in Fig. 2 clearly blueshifts for high pair densities: this means that the overall spectral shift cannot be merely assigned to band filling or to some saturation of localized states. It is mainly due to the screening of the field.

The large amplitude of the present spectral shift makes it impossible to use the classical procedure for measuring the time-dependent PL intensity, which is usually taken at a fixed photon energy. Instead, we need to plot as a function of time [Fig. 3(c)], the integrated area of the Gaussian curves that we used to fit the time-dependent spectra. In this figure, we do not present the data points that correspond to times during the excitation pulse, since we want to observe the relaxation behavior of the system after the excitation. The decay of the intensity is clearly nonexponential and this can easily be explained by a decrease of the radiative time due to the screening effect at shorter delays. The electron and hole wave func-

tion overlap integral is enhanced at the beginning of the phenomenon due to the screening of the electric field and progressively decreases as the electron-hole pair density decreases.

IV. THEORETICAL MODEL

To try to describe our experimental data theoretically, we self-consistently solve the Schrödinger and Poisson equations, within the envelope function approximation. By doing so, we calculate the electron and hole wave functions and energy levels by taking into account the modifications on the well potential profile caused by the accumulation of carriers in the well. The basic equations and numerical parameters for the present strained materials are available in Ref. 49, where the changes of the entire absorption spectrum of a GaN/(Al,Ga)N QW, under high excitation, are calculated. Here, we will restrict ourselves to the energy and oscillator strength of the ground-state (so-called $E1$-$H1$) optical transition. Using the two-dimensional densities of states, proportional to the appropriate in-plane effective masses, we calculate the population of each subband and the quasi-Fermi levels, for electrons and holes. Given the population of each subband, we calculate the modification of the potential by solving Poisson's equation

$$\frac{d^2V}{dz^2} = -\frac{\rho(z)}{\varepsilon\varepsilon_0}, \tag{1}$$

where $\rho(z)$ is the charge density profile given by

$$\rho(z) = e\sum_{i,j}\,[n_{hi}|f_{hi}(z)|^2 - n_{ej}|f_{ej}(z)|^2]. \tag{2}$$

Here, $f_{e,h,i,j}(z)$ are the envelope functions for the electrons and holes in the well, and $n_{e,h,i,j}$ are the carrier populations for each subband i and j. Moreover,

$$n = \sum_i\, n_{hi} = \sum_j\, n_{ej}, \tag{3}$$

where n is the total density of *e-h* pairs. In practice, for the system and the densities considered here, we found that only the first subbands ($i=j=1$) were populated. By using Eqs. (2) and (3), we account for the charge distribution induced by the population of the ground states. Energy levels and envelope functions are determined by using a finite-element technique. With this method, the details of the band curvature induced by the charge accumulation are obtained self-consistently, yielding a curved potential profile. This is more accurate, especially concerning the oscillator strengths, than calculating an effective screening field, thus keeping a triangular band profile.

In order to include the band-gap renormalization which results from carrier-carrier scattering (many-body) effects, we use the results of previous work.[40] The band-gap renormalization redshifts the optical transition by a quantity ΔE_G that follows a kind of "universal" law, which can be fitted by

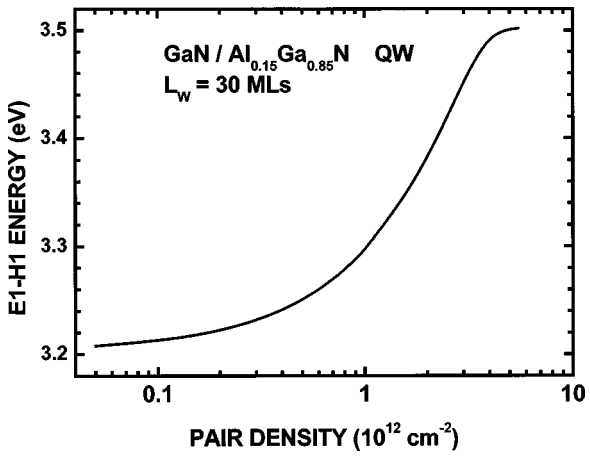

FIG. 4. Calculated PL energies as a function of the density of *e-h* pairs.

$$\frac{\Delta E_G}{R_{2D}} = -1.67(r_{2D})^{-0.71}, \tag{4}$$

where R_{2D} is the binding energy of two-dimensional excitons, i.e., four times the three-dimensional value for GaN ($R_{2D}=0.1$ eV) and r_{2D} the so-called "dimensionless interparticle distance," which is deduced from the exciton two-dimensional Bohr radius $a_B^{2D}=0.5\,a_B^{3D}$, via $r_{2D}=1/[\pi n(a_B^{2D})^2]^{1/2}$, where $a_B^{2D}=1.5$ nm, for GaN.

The band-filling effects are also included: we consider the "basic" $E1$-$H1$ transition energy as resulting from the screening and BGR, and the "uppermost" energy as the latter augmented by the sum of the pdeudo-Fermi energies for electrons and holes. We estimate the energy position of our PL peak as being exactly in the middle of these two extremes. We neglect excitonic effects for the reasons discussed above and because it has been established earlier[36] that the exciton binding energy goes to zero for carrier densities of a few 10^{11} cm^{-2}, lower by one order of magnitude than those considered here.

The maximum value of the electric field in the well was estimated by using the following formula:[6] $F_{\max}(x)=\beta x$, where x is the aluminum concentration and $\beta=5.5$ MV/cm. In practice, we need to account for the distribution of the polarizations between the well (width L_W) and the barrier (width L_B), so that the field in the QW, F_W, is given by[46] $F_W=F_{\max}L_B/(L_B+L_W)$. We find a value of $F_W=670$ kV/cm. Using this value, we calculate an $E1$-$H1$ transition energy, for the "unscreened" case, of 3.21 eV, that agrees well with the experimental transition energy that we find at large delays.

In practice, we have calculated the dependence of the transition energy (Fig. 4) and of the squared overlap integral I (Fig. 5) on the density of *e-h* pairs, n. To produce the energy variation of Fig. 3, n had to be varied up to a few times 10^{12} cm^{-2}. Above 4×10^{12} cm^{-2}, the transition energy saturates near 3.50 eV because the system nearly reaches the flatband situation. The corresponding variation of I is much more dramatic: when n goes from zero to 5.5×10^{12} cm^{-2}, I is increased from $\sim2\times10^{-4}$ to 0.85.

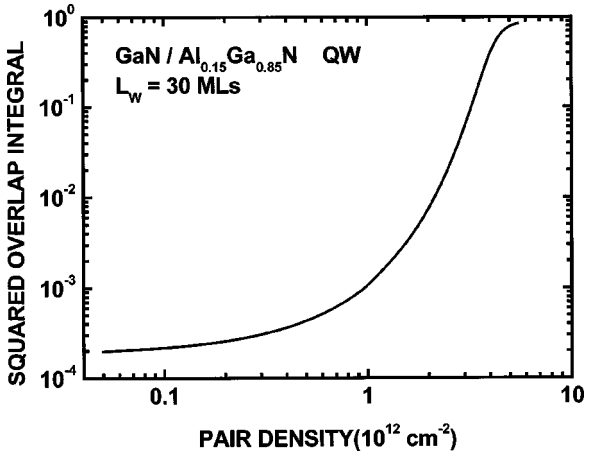

FIG. 5. Calculated squared overlap integral of electron and hole envelope functions, as a function of the density of pairs.

Since the radiative recombination time is inversely proportional to I, we see that the recombination rate can be decreased over nearly four orders of magnitude during the entire relaxation process, if we start from extremely high *e-h* pair densities.

To reproduce the overall recombination dynamics, we used the finite-element method that allowed us to calculate the change in n from

$$\frac{dn}{dt} = -\frac{n}{\tau(n)}, \tag{5}$$

where τ is the radiative time given by

$$\tau(n) = \frac{I_0}{I(n)}\,\tau_0. \tag{6}$$

I_0 is the squared overlap integral in the unscreened case (where the pair density is zero), and $I(n)$ is the squared overlap integral for the pair density n. In Eq. (6), τ_0 corresponds to the radiative lifetime for the carriers in the well for the unscreened case. Given an initial pair density $n(t=0)$, which is easily determined from the experimental initial emission energy, the time evolution of n is then evaluated for a succession of elementary intervals of time. For each interval, the elementary change δn is evaluated from Eq. (5) and from the values of n and $\tau(n)$ [from Eq. (6)] in the previous time interval. This provides the overall time dependence of both the $E1$-$H1$ energy and the quantity dn/dt, which is proportional to the emission intensity, if nonradiative recombination is neglected.

V. DISCUSSION

In order to model our experimental results with this approach, we had to restrict ourselves to the situation where there is no carrier generation, i.e., to times where the excitation pulse is not present. For this reason, we limit our time range to delays larger than ~5 ns, from the time of maximum laser excitation. We wish to emphasize the fact that the asymptotic situation for $t\to\infty$ was calculated *with no adjustable parameter*: the electric field, and thus the asymptotic transition energy, and the asymptotic radiative lifetime of $\tau_0 = 1.65\ \mu$s were all deduced from previous work,[5,6,44] as already mentioned. In these conditions and for the laser power density used in the experiment of Figs. 1–3, the only parameter is the pair density left in the QW after the end of the laser pulse: as shown in Figs. 3(a) and 3(c), we obtained an excellent agreement between our calculation and experimental data with $n(t=0) = 2.9\times10^{12}$ cm^{-2}.

The finite-element model agrees very well with the experimental time dependence of the PL energy: we thus correctly calculate the complex time dependence of the pair density n. The main part of the energy shift that is observed takes place within a few tens of nanoseconds, even with a τ_0 of a few microseconds. The reason for this is the large change of the overlap integral with n that can be produced in such a wide quantum well, and which we correctly calculate. The overlap integral for $n = 3\times10^{12}$ cm^{-2} is 0.05 whereas it is 2×10^{-4} for the unscreened case. This means that, in our experiment, the radiative time ''constant'' of the system starts with a small value (we calculate $\tau\sim8$ ns for $t=1$ ns *after the end* of the pulse) and progressively increases as the *e-h* recombination takes place. In fact, τ does not reach the value of τ_0, even after a delay of 200 ns, where it is only 0.42 μs, since we calculate that there is still a pair density of $\sim8\times10^{11}$ cm^{-2} left in the well at that time. By the way, the latter value proves that we can still neglect the excitonic interaction for this delay.[36,37]

Concerning the PL intensity, our model gives a satisfactory description of the nonexponential time dependence of Fig. 3(c). However, for delays larger than ~100 ns, the experimental intensity is smaller than the calculated value. Possible reasons for this small discrepancy are as follows.

(1) The loss of accuracy on the measurement of the area of the fitting Gaussian curve, at large delays, where the signal-to-noise ratio becomes very small; this problem is less crucial for the pointing of the maximum PL energy.
(2) The presence of relatively slow nonradiative recombination channels, which are not dominant when the radiative lifetime is small (shorter delays), but may become important at larger delays, where it becomes difficult to measure a reliable PL signal. This interference of nonradiative channels has already been discussed[41–44] in the analysis of the decay dynamics of similar GaN/AlGaN QWs. It was found to reduce significantly the excitonic lifetime for multiple QWs with narrow barriers,[44] which is not the case here. The overall agreement that we obtain proves that the nonradiative recombination mechanisms are not of crucial importance for the beginning of the relaxation, when the radiative recombination is fast enough. After 100–150 ns, this situation may change, considering the very large radiative lifetime.
(3) However, we should not forget the uncertainty of basic numerical parameters (electric field, effective masses, band offsets, exact strain of the well and barrier layers, and so on) and some approximations made (see above), to which the calculation of the energy is obviously less

sensitive than the calculation of the recombination rate. This is not surprising, since the latter depends on the calculation of the overlap integral of envelope functions, which vary over several orders of magnitude, and which is known to be more ''delicate'' than the calculation of the energy.

By adjusting some parameters, such as the asymptotic time constant or the electric field, we would certainly refine the agreement between our model and our results. But we believe that this kind of fitting procedure is pointless, especially when we consider the excellent result provided with a single adjustable parameter.

VI. CONCLUSION

By using the fourth harmonic of a high-power, pulsed YAG laser, we succeeded in screening the internal electric field of a $GaN/Al_{0.15}Ga_{0.85}N$ QW. We did this with an amplitude of induced blueshift that leaves no doubt about the nature of the mechanism involved. In particular, other effects, like, e.g., the screening of the excitonic interaction, can be ignored in first approximation, since they are obviously smaller by one order of magnitude than the 0.2 eV shifts that we measured. An excellent fit to the time-dependent transition energy is obtained by using as the only fitting parameter the initial density of *e-h* pairs. The asymptotic time constant of $\tau_0 = 1.65\ \mu s$ was fixed by a scaling procedure based on previous studies of narrower QWs. We can conclude that the overall dynamics, in the present experiments, is well described by a finite-element treatment, including our self-consistent solution of the Poisson and Schrödinger equations. In particular, the change of dynamics with time is well described by a change of the *e-h* envelope function overlap integral that we calculate. The nonexponential intensity decay is also well accounted for by our modeling.

[1] A. Bykhovsky, B. L. Gelmont, and M. Shur, J. Appl. Phys. **81**, 6332 (1997).

[2] Jin Seo Im, H. Kollmer, J. Off, A. Sohmer, F. Scholz, and A. Hangleiter, Phys. Rev. B **57**, R9435 (1998).

[3] F. Bernardini, V. Fiorentini, and D. Vanderbilt, Phys. Rev. B **57**, R9427 (1998).

[4] F. Bernardini, V. Fiorentini, and D. Vanderbilt, Phys. Rev. B **56**, R10 024 (1997).

[5] M. Leroux, N. Grandjean, J. Massies, B. Gil, P. Lefebvre, and P. Bigenwald, Phys. Rev. B **60**, 1496 (1999).

[6] N. Grandjean, J. Massies, and M. Leroux, Appl. Phys. Lett. **74**, 2361 (1999).

[7] E. Berkowicz, D. Gershoni, G. Bahir, E. Lakin, D. Shilo, E. Zolotoyabko, A. C. Abare, S. P. DenBaars, and L. A. Coldren, Phys. Rev. B **61**, 10 994 (2000).

[8] T. Takeuchi, S. Sota, M. Kasturagawa, M. Komori, H. Takeuchi, H. Amano, and I. Akasaki, Jpn. J. Appl. Phys., Part 2 **36**, L382 (1997).

[9] C. Wetzel, T. Takeuchi, H. Amano, and I. Akasaki, Phys. Rev. B **62**, R13 302 (2000).

[10] P. Lefebvre, A. Morel, M. Gallart, T. Taliercio, J. Allègre, B. Gil, H. Mathieu, B. Damilano, N. Grandjean, and J. Massies, Appl. Phys. Lett. **78**, 1252 (2001).

[11] C. Adelmann, S. Fanget, E. Sarigiannidou, D. Jalabert, Y. Hori, T. Shibata, M. Tanaka, J.-L. Rouvière, C. Bru-Chevallier, and B. Daudin, Appl. Phys. Lett. **82**, 4154 (2003).

[12] D. L. Smith and C. Mailhiot, Rev. Mod. Phys. **62**, 173 (1990).

[13] P. Boring, K. J. Moore, P. Bigenwald, B. Gil, and K. Woodbridge, J. Phys. IV **3**, C5-249 (1993).

[14] P. Boring, B. Gil, and K. J. Moore, Phys. Rev. Lett. **71**, 1875 (1993).

[15] R. André, J. Cibert, and Le Si Dang, Phys. Rev. B **52**, 12 013 (1995).

[16] F. Renner, P. Kiesel, and G. H. Döhler, M. Kneissl, C. G. Van de Walle, and N. M. Johnson, Appl. Phys. Lett. **81**, 490 (2002).

[17] N. Grandjean, B. Damilano, S. Dalmasso, M. Leroux, M. Laügt, and J. Massies, J. Appl. Phys. **86**, 3714 (1999).

[18] S. Schmitt-Rink, D. S. Chemla, and D. A. B. Miller, Phys. Rev. B **32**, 6601 (1985).

[19] S. Schmitt-Rink, D. S. Chemla, and D. A. B. Miller, Adv. Phys. **38**, 89 (1989).

[20] P. W. Smith, Y. Silberberg, and D. A. B. Miller, J. Opt. Soc. Am. B **2**, 1228 (1985).

[21] D. S. Chemla, D. A. B. Miller, and S. Schmitt-Rink, Phys. Rev. Lett. **59**, 1018 (1987).

[22] M. Yamanishi, Phys. Rev. Lett. **59**, 1014 (1987).

[23] W. H. Knox, D. S. Chemla, D. A. B. Miller, J. B. Stark, and S. Schmitt-Rink, Phys. Rev. Lett. **62**, 1189 (1989).

[24] S. Schmitt-Rink and D. S. Chemla, Phys. Rev. Lett. **57**, 2752 (1986).

[25] K. J. Moore, P. Boring, B. Gil, and K. Woodbridge, Phys. Rev. B **48**, 18 010 (1993).

[26] H. S. Kim, J. Y. Lin, H. X. Jiang, W. W. Chow, A. Botchkarev, and H. Morkoç, Appl. Phys. Lett. **73**, 3426 (1998).

[27] T. Kuroda, A. Tackeuchi, and T. Sota, Appl. Phys. Lett. **76**, 3753 (2000).

[28] R. Cingolani, A. Botchkarev, H. Tang, H. Morkoç, G. Traetta, G. Coli, M. Lomascolo, A. Di Carlo, F. Della Sala, and P. Lugli, Phys. Rev. B **61**, 2711 (2000).

[29] G. H. Gainer, Y. H. Kwon, J. B. Lam, S. Bidnyk, A. Kalashyan, J. J. Song, S. C. Choi, and G. M. Yang, Appl. Phys. Lett. **78**, 3890 (2001).

[30] E. Kuotskis, J. Zhang, M.-Y. Ryu, J. W. Yang, G. Simin, M. Asif Khan, R. Gaska, and M. S. Shur, Appl. Phys. Lett. **79**, 4375 (2001).

[31] E. Kuokstis, C. Q. Chen, M. E. Gaevski, W. H. Sun, J. W. Yang, G. Simin, M. Asif Khan, H. P. Maruska, D. W. Hill, M. C. Chou, J. J. Gallagher, and B. Chai, Appl. Phys. Lett. **81**, 4130 (2002).

[32] E. Kuokstis, J. W. Yang, G. Smith, M. Asif Khan, R. Gaska, and M. S. Shur, Appl. Phys. Lett. **80**, 977 (2002).

[33] S. P. Lepkowski, T. Suski, P. Perlin, V. Yu. Ivanov, M. Godlewski, N. Grandjean, and J. Massies, J. Appl. Phys. **91**, 9622 (2002).

[34] T. Kuroda and A. Tackeuchi, J. Appl. Phys. **92**, 3071 (2002).

[35] A. Reale, G. Massari, A. Di Carlo, P. Lugli, A. Vinattieri, D.

Alderighi, M. Colocci, F. Semond, N. Grandjean, and J. Massies, J. Appl. Phys. **93**, 400 (2003).
[36] P. Bigenwald, A. Kavokin, B. Gil, and P. Lefebvre, Phys. Rev. B **63**, 035315 (2001).
[37] P. Bigenwald, A. Kavokin, B. Gil, and P. Lefebvre, Phys. Rev. B **61**, 15 621 (2000).
[38] G. Bastard, *Wave Mechanics Applied to Semiconductor Hetereostructures* (Les Editions de Physique, Les Ulis, France, 1988).
[39] S. H. Park and S.-L. Chuang, Appl. Phys. Lett. **72**, 287 (1998).
[40] S. H. Park and S.-L. Chuang, Appl. Phys. Lett. **76**, 1981 (2000).
[41] A. Reale, A. Di Carlo, P. Lugli, and A. Kavokin, Phys. Status Solidi A **183**, 121 (2001).
[42] A. Reale, G. Massari, A. Di Carlo, and P. Lugli, Phys. Status Solidi A **190**, 81 (2002).
[43] A. Di Carlo and A. Reale, Phys. Status Solidi B **228**, 553 (2001).
[44] P. Lefebvre, M. Gallart, T. Taliercio, B. Gil, J. Allègre, H. Mathieu, N. Grandjean, M. Leroux, J. Massies, and P. Bigenwald, Phys. Status Solidi B **216**, 361 (1999).
[45] A. Bellabchara, P. Lefebvre, P. Christol, and H. Mathieu, Phys. Rev. B **50**, 11 840 (1994).
[46] M. Leroux, N. Grandjean, M. Laügt, J. Massies, B. Gil, P. Lefebvre, and P. Bigenwald, Phys. Rev. B **58**, R13 371 (1998).
[47] P. Lefebvre, J. Allègre, B. Gil, H. Mathieu, N. Grandjean, M. Leroux, J. Massies, and P. Bigenwald, Phys. Rev. B **59**, 15 363 (1999).
[48] M. Gallart, P. Lefebvre, A. Morel, T. Taliercio, B. Gil, J. Allègre, H. Mathieu, B. Damilano, N. Grandjean, and J. Massies, Phys. Status Solidi A **183**, 61 (2001).
[49] S. Kalliakos, P. Lefebvre, and T. Taliercio, Phys. Rev. B **67**, 205307 (2003).